Civil Engineering Beyond Limits 2 (2024) 1927
Civil Engineering Beyond Limits
journal home: www.acapublishing.com/journals/1/cebel
Research Article

Damage Diagnosis in RC Frames on a Frequency Domain Basis

Oğuzhan Çelebi*,[1], Mahmut Kılıç[1], Abdulkadir Cüneyt Aydın[1]
[1]*Ataturk University, Engineering Faculty Civil Engineering Department, Erzurum, Turkey*

Keywords

Damage diagnosis,
Frequency domain,
Pushover analysis,
Reinforced concrete.

Abstract

Today, there are many methods for detecting damages in reinforced concrete structures, such as pushover analysis, energy-based analysis and nonlinear analysis in the time domain. These methods are used to determine the dynamic properties of the structure by using accelerometers and a number of measuring devices that determine the mechanical and physical properties of the structure. In this study, it is aimed to diagnose damage with a set of frequencies and corresponding amplitude values obtained from accelerometers that determine the dynamic properties of the structure, instead of these methods that create calculation complexity. In this study, firstly, the damaged elements and joint points of the 1-storey RC frame with a single opening in both directions were determined by pushover analysis, for which the finite element model was built in the SAP2000 program. Later, time history analyzes were carried out under the influence of acceleration data of the Pazarcık earthquake (Mw 7.7) that occurred on February 6. The results obtained in the time domain were converted into the frequency domain and some inferences were made regarding the damaged areas. The study results showed that if the amplitude drop decreases in the same frequency range at a node, damage occurs at that node. It has been determined that the damages occurring in the RC frame increase due to the decrease in amplitude.

1. Introduction

Nowadays, performance-based analyzes are performed to determine the condition of existing structures before and after earthquakes [1]. As a result of these analyses, existing structures are repaired/reinforced and demolished. From this perspective, it is concluded that performance-based analyzes are very important. Many different analysis methods have been developed for the performance analysis of existing structures accepted in the literature and the scientific world [2-3]. These analysis methods are nonlinear static pushover analysis and nonlinear analysis in time domain [2-3]. In these two methods, limited, controlled and collapse prevention performance levels of structures are obtained depending on deformation [4]. Pushover analysis for seismic evaluation of reinforced concrete structures has been investigated in many studies [5-7]. However, in order to obtain accurate results from these methods, building material determination, structural element geometries and soil determination information are needed. Rapid damage assessment techniques have been developed for existing structures before and after earthquakes [5-7]. Finding earthquake damages not only through the mainshock but also by including aftershocks is an important parameter. Li et al. (2014) developed a damage detection method by developing a scaling method that combines mainshocks and aftershocks. The results of the study showed that with this method, more damage occurred than the damage caused by mainshocks [8]. Demirbaş vd. (2022) studied the energy-based assessment approach for determining the performance level of reinforced concrete structures [9]. Kosarzadeh and Poursha (2023) used modal pushover analysis (MPA), consecutive modal pushover (CMP) procedure, extended N2 (EN2) method, single-run multi-mode pushover (SMP) method and non-adaptive displacement-based pushover (NADP) method for seismic evaluation of vertically irregular reinforced concrete frames subjected to main shock- aftershock sequences of near fault and far fault ground motions [10]. Kim vd. (2023) used the pushover analysis method to determine the performance levels of low-rise pilot buildings after the 2017 Pohang earthquake [11]. Zhou et al. (2023) determined the seismic evaluation of the reinforced concrete structure by using pushover analysis, taking into account the earth fissure. Joseph et al. (2023) tested the accuracy of the flexural and shear behavior of a reinforced concrete structure using pushover analysis with shake table experiments [12]. Peng et al. (2023) determined the drift story drift ratio limit values and lateral load resistance of reinforced concrete frames using pushover analysis [13].

In addition to methods such as pushover analyses, seismic evaluations of existing structures are also carried out with the use of structural health monitoring (SHM) technologies. Building health monitoring in existing structures is generally applied as vibration analysis, vision-based systems, impedance-based techniques and optical fiber technologies [14-17]. With structural health monitoring methods, structural damages can be determined by calculating natural frequencies, modal damping, mode shapes and strain energies derived from them [18-22]. Such systems, defined for the evaluation of existing structures, are considered to be a suitable solution for faster damage diagnosis. However, such applications have some difficulties in terms of requiring expertise and choosing the right calculation approaches. Structural health monitoring systems are generally used to detect global damages. Detecting local damages within the framework of some seismic effects is also an important issue. In addition, some complex calculation procedures need to be simplified to detect local and global damage types. Li et al. (2012) developed innovative approaches in the frequency time domain recognition to detect damages in infrastructures [23]. Beyen 2021 has developed a method in the frequency domain (T-F Domain) for damage diagnosis in historical masonry structures. In this study, local damage was estimated [24]. Perez et al. (2021) evaluated the structural damage of lattice towers based on the frequency domain correlation approach [25]. The results showed a correlation between the proposed spectral correlation indices (SCI) and changes in stiffness and mass in the lattice tower [25]. Auersch examined the resonance possibility of the railway structure by relating it to the frequency domain [26]. Song et al. (2024) compared the damage caused by vibrations in viaducts by examining them in the time history and frequency domain. The study

*Corresponding Author: celebioguzhan@atauni.edu.tr
Received 05 Jul 2024; Revised 15 Jul 2024; Accepted 15 Jul 2024
https://doi.org/10.36937/cebel.2024.1927
2687-5756 /

results showed that damage simulations caused by vibrations in the frequency domain were successfully achieved [27].

In the current study, it is aimed to detect damage by finding the frequency domain equivalents of vibrations occurring in existing structures by using accelerometers. For this purpose, numerical analysis method was preferred first. In this context, firstly, the performance level of the reinforced concrete frame was examined in the frequency domain. Performance analysis was made with single-mode pushover analysis applied to the reinforced concrete frame. As a result of the performance analysis, the relevant node points of the damaged and undamaged structural elements were determined. Then, analyzes were applied in the time domain under the influence of the Kahramanmaraş-centered Pazarcık earthquake (7.7 Mw) data on February 6, 2022. Response acceleration data taken from damaged and undamaged nodes were converted into frequency domain. The T-F values obtained at the joints were compared with the moment-rotation damage limit values in the pushover analysis results and their connection with each other was determined.

2. Material and Method

In this study, damage diagnosis was made on a two-storey reinforced concrete frame. The finite element model of the frame, the dimensions of which are given in Figure 1, was established in the computer-aided SAP2000 program, shown in Figure 2. The floor height of the reinforced concrete frame is designed as 3.00 m, the span in one direction is 5.50 m and the span in the other direction is 6.00 m. The column size of the frame is 30x50 cm and the beam size is 25x50 cm. The longitudinal reinforcements corresponding to these dimensions are designed as 8Φ16 and 6Φ14 respectively. Transverse reinforcement in columns and beams is considered as Φ10/10/15/10. Bearing element dimensions and reinforcement are regulated according to the Turkish Building Earthquake Code 2018 [4].

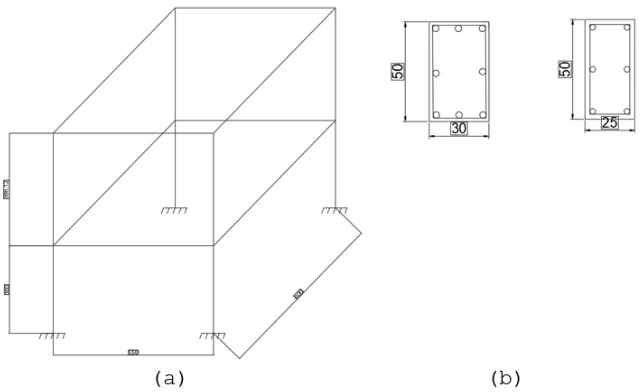

Figure 1. Reinforced concrete frame; a) perspective view, b) Reinforcement bar detail

In accordance with TBEC 2018, the floor thickness was taken as 15 cm. According to the TS498 specification, a dead load of 4 kN/m was applied to the walls, a dead load of 3 kN/m^2 and a live load of 2 kN/m^2 was applied to the slabs. The weight of the structure is defined in the G+0.3Q load combination [28].

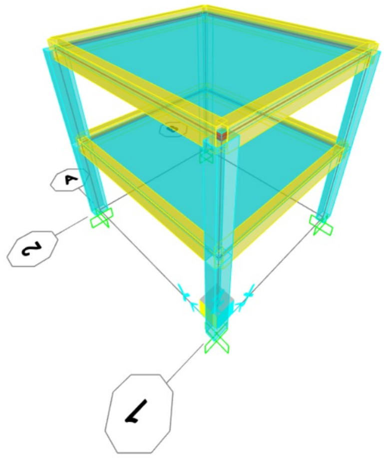

Figure 2. The finite element model of the reinforced concrete frame

The cross-sections of the load-bearing elements are designed as shown in Figure 3, according to their size and reinforcement placement. Moment-curvature diagrams for columns and beams were prepared for structural analysis.

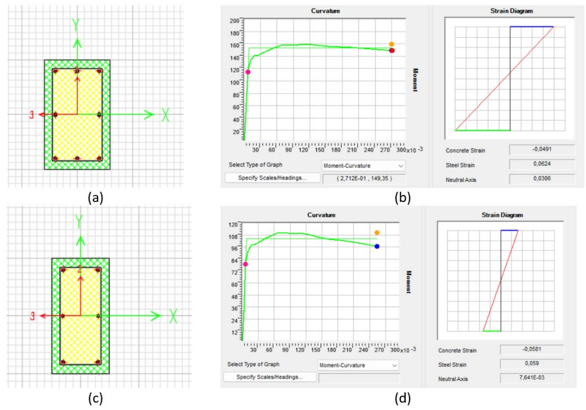

Figure 3. The informations cross-sections of column and beam; a) column cross section, b) moment-curvature of column, c) beam cross section, d) moment curvature of beam

According to Figure 3, the moment values at the moment of yielding for columns and beams are calculated to be approximately 148 and 106 kNm, respectively. The curvature values at yield and rupture corresponding to these values are 0.00865 and 0.269 for the column, respectively. The curvature values for the beam at yield and rupture were calculated as 0.00673 and 0.252, respectively.

After establishing the finite element model of the reinforced concrete frame, single-mode performance analysis was applied. For performance analysis, P-M2-M3 (Axial pressure force and bending in both directions) plastic joints were defined for the columns. M3 (simple bending) joints are defined in the beams. Then, performance analysis was made by applying static pushover analysis in one direction. TBEC 2018 was also used in the application of performance analysis criteria. In the performance analysis, first the static thrust curve (base shear force-peak displacement curve) was obtained, and then the pseudo displacement and pseudo acceleration curves were obtained depending on this curve. Performance points were obtained by plotting this curve together with the horizontal elastic acceleration and displacement curve of the reinforced concrete frame. Performance evaluation was made according to the unit strain and rotation values of the structural elements according to the performance points. The rotation values calculated as a result of the performance analysis were converted into curvature values according to TBEC 2018 criteria. The curvature values obtained as a result of the analysis were placed in the moment-curvature diagram shown in Figure 3 and the corresponding strain values were calculated for concrete and reinforcement. According to these calculated values, the performance levels of the building elements were obtained according to TBEC 2018.

The reinforced concrete frame that is the subject of the study is thought to be located at 39.90942 Latitude and 41.224666 Longitude within the Erzurum Province of Turkey. According to TBEC 2018 criteria, ZD (Multilayer clay layers) soil class was accepted and local earthquake parameters were determined according to DD-1 and DD-2 earthquake movement levels and are shown in Table 1. These values are important parameters that will be used to determine how much the earthquake will affect the structure. By using the values in Table 1, the horizontal elastic acceleration spectrum of the structure was obtained for the DD-2 earthquake ground motion level (Figure 4). Earthquake records to be used in structural analysis are scaled according to the horizontal elastic acceleration spectrum. Horizontal elastic acceleration spectrum is an important curve that reveals the earthquake risk of a structure.

Table 1. Local earthquake parameters [29]

Earthquake ground motion level	S_{DS}	S_{D1}	S_S	S_1	PGA (g)
DD-1	1.820	0.480	1.820	0.480	0.730
DD-2	1.079	0.544	0.971	0.261	0.407

In Table 1, DD-1 represents the earthquake ground motion level with a 2% probability of being exceeded in 50 years (recurrence period of 2475 years), and DD-2 represents the earthquake ground motion level with a 10% probability of being exceeded in 50 years (recurrence period of 2475 years). SDS represents the short period design spectral acceleration coefficient, SD1 represents the design spectral acceleration coefficient for the 1.0 second period, SS represents the Short period map spectral acceleration coefficient, S1 represents the map spectral acceleration coefficient for the 1.0 second period, and PGA represents the peak ground acceleration [4, 29].

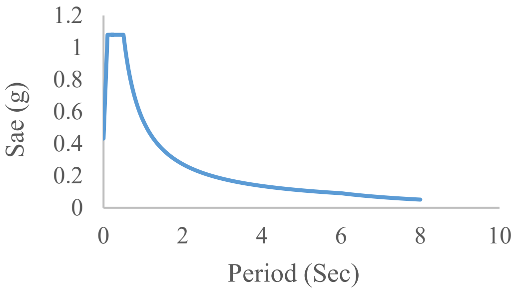

Figure 4. Horizontal elastic acceleration spectrum of the structure

After the performance evaluation determined by static pushover analysis, time history analyzes were applied. For analyzes in the time domain, acceleration data of the Pazarcık earthquake (Mw 7.8) that occurred on 06.02.2023 were used (Figure 5). According to AFAD (Ministry of Internal Affairs Disaster and Emergency Management Presidency) data, Pazarcık earthquake has the peak ground acceleration (PGA) of 2.004g.

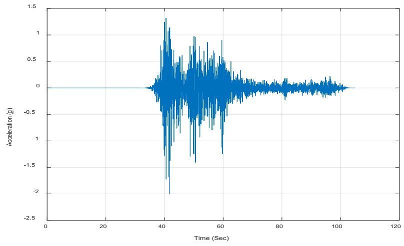

Figure 5. Time history of Pazarcık earthquake

The spectrum of Pazarcık earthquake was obtained according to the basic principles of Structural Dynamics [30-31] and plotted together with the horizontal elastic acceleration spectrum as shown in Figure 6. According to TBEC 2018 criteria, earthquake spectrum acceleration values that are much higher than the spectrum acceleration values in the effective period intervals (0.2Tp-1.5Tp) of the horizontal elastic acceleration spectrum have been scaled (Figure 6). Based on the scaled earthquake spectra, the acceleration values to be used for analysis in the time domain were scaled and plotted over time as shown in Figure 6.

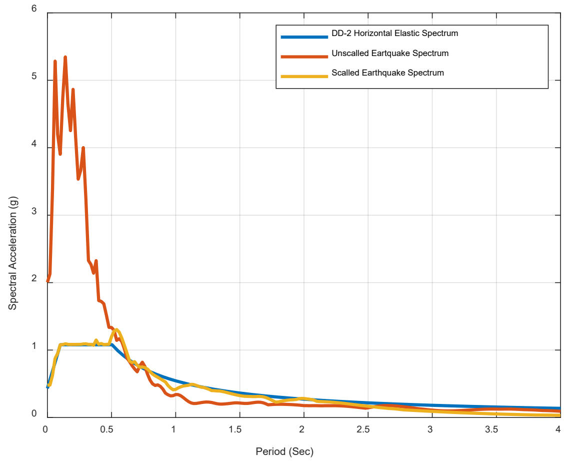

Figure 6. Spectrum curves

In Figure 6, the maximum acceleration value of the horizontal elastic acceleration spectrum is 1.08g, and the acceleration values of the unscaled and scaled earthquake spectrum are 5.34g and 1.304g, respectively. In Figure 7, it was determined that the original peak ground acceleration value was 2.004g and the scaled peak ground acceleration was 0.480g. In this case, the earthquake acceleration record to be used in the structure analysis has been proven to be scaled according to TBEC 2018. The earthquake acceleration record was completed in the SAP2000 program and was made ready for analysis.

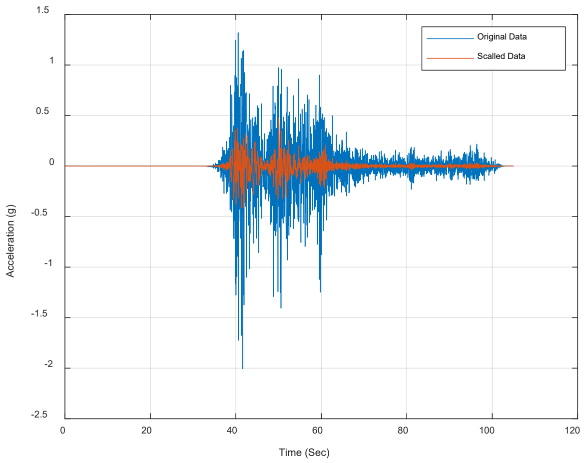

Figure 7. Time history of original and unscaled data

Acceleration values of limited damage (IO), significant damage (LS) and collapse (CP) damage points to be obtained as a result of the performance analysis were taken in the time domain. These acceleration values were then solved in the frequency domain and associated with damage levels. The study was concluded by establishing relationships between frequency content, acceleration and damage.

3. Analysis Results

In this study, damage diagnosis was made in the frequency domain on a two-story reinforced concrete frame. Modal analysis results are given in Table 1.

Table 1. The modal analysis results

T1	T2	T3	UX	UY	UZ
0.527	0.419	0.376	0.915	0.915	0.890

In Table 1, T1, T2 and T3 represent the 1st, 2nd and 3rd mode periods, respectively. In addition, UX, UY and UZ represent the mass participation rates in the X, Y and Z directions, respectively. Modal analysis results showed that the failure mode of the frame was bending. Static pushover analysis was performed unimodally in the X direction. After the modal analysis, static pushover analysis was applied to the frame. The static pushover curve is obtained in Figure 8.

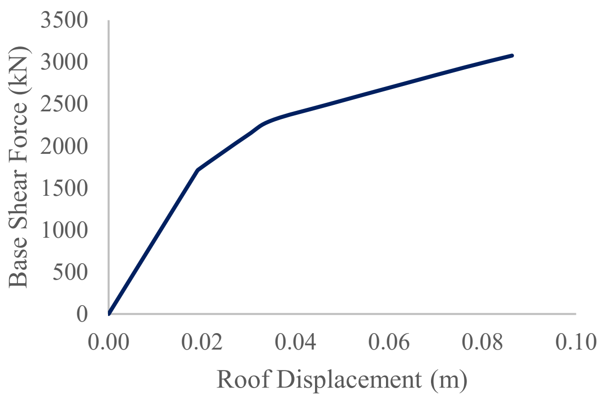

Figure 8. The static pushover curve for structure frame

According to Figure 8, it was calculated that 3078 kN base shear force and 0.0862 m peak displacement occurred in the reinforced concrete frame. According to the effective mass and modal parameters of the frame, the pseudo displacement and acceleration curve was obtained and matched with the horizontal elastic acceleration spectrum and spectral displacement curve as shown in Figure 9. According to Figure 9, the performance point of the structure was determined to be 0.0290 m and 0.37g. In the structural analysis, the successive thrust step was terminated at 0.0290 m displacement. And according to this performance value, the performance level of the building elements was determined.

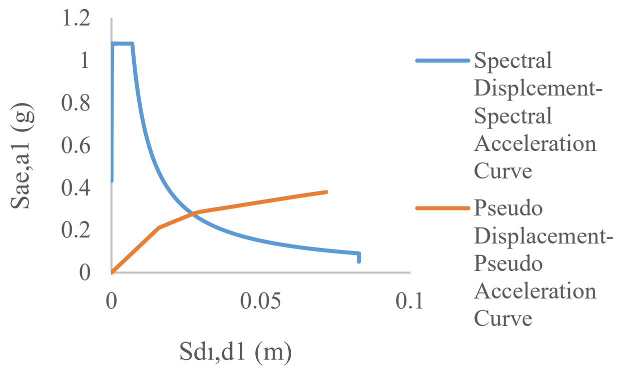

Figure 9. Performance points of structural frame

As shown in Figure 10, it was determined that there was damage to the 1st floor columns and beams of the reinforced concrete frame, but no damage occurred to the second floor load-bearing elements.

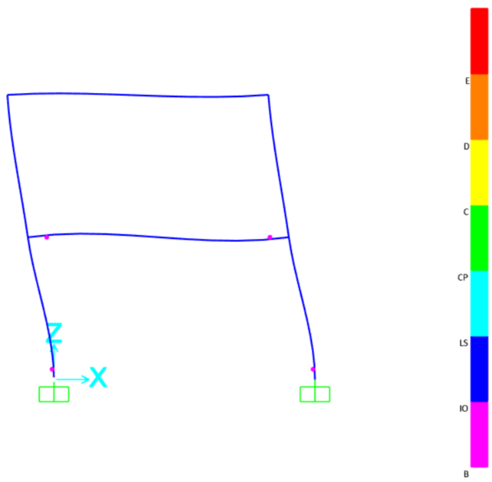

Figure 10. Damaged carrier members

A rotation of 0.00324 (Figure 11a) occurred at the damaged node of the 1st floor, and 0.00194 rotation (Figure 11b) occurred at the nodal point of the 2nd floor, which was not damaged. It has been confirmed that the damages become more evident with increasing rotation values. It was determined that the rotation value occurring at the undamaged node on the 1st floor was 0.00242.

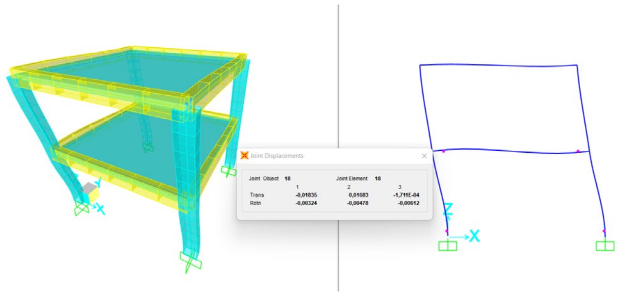

(a)

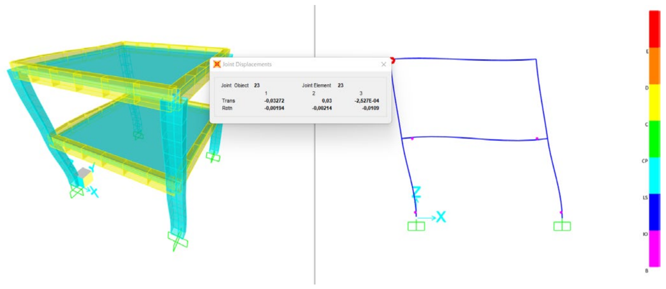

(b)

(c)

Figure 11. Rotation values for structural nodes; a) first floor, b) second floor, c) first floor node that was not damaged

The moment rotation curve of the node shown in Figure 11a is given in Figure 12. The moment rotation curve of the node given in Figure 11b is given in Figure 13. It was concluded that in the undamaged case, the moment rotation curve behaves ideally as shown in Figure 3, but the moment rotation curve in Figure 12 is not ideal. It has been determined that the building element has collapsed.

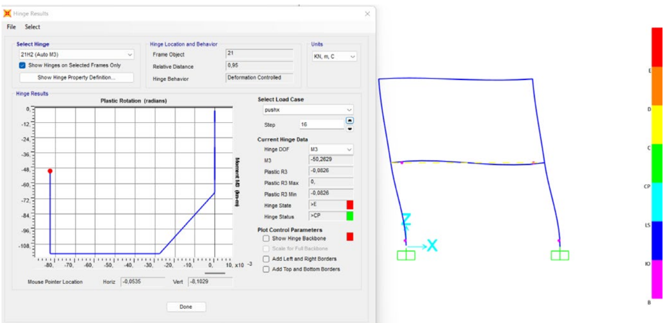

Figure 12. Moment-rotation curve for damage nodes

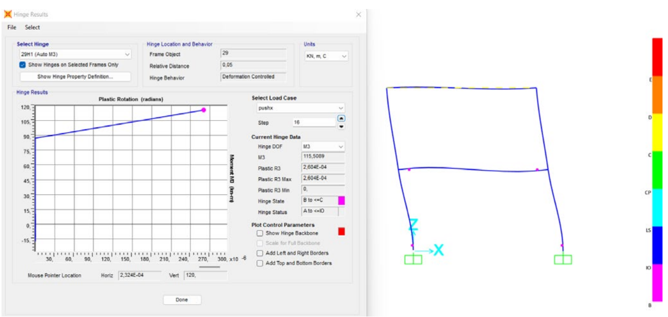

Figure 13. Moment-rotation curve for non-damaged nodes

After determining the performance levels in the static pushover analysis, analyzes were applied in the time domain. As shown in Figure 14, an acceleration value of approximately 1g occurred at the undamaged node, while an acceleration value of approximately 0.5g occurred at the damaged node. This situation is explained by the fact that the damaged node oscillates less against the earthquake and dissipates insufficient energy.

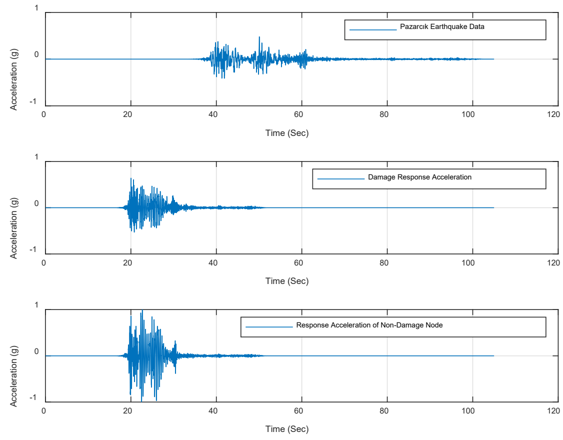

Figure 14. The analysis results in the time domain

The data obtained at damaged and undamaged nodes were solved in the frequency domain using Fourier techniques as shown in Figure 15.

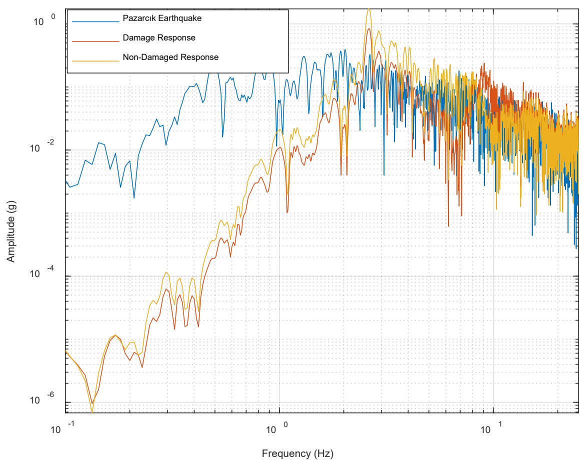

Figure 15. Frequency time domain results

It has been observed that the damaged structure oscillates in different directions with the earthquake direction in the weak axis mode. It is shown that the damaged node has sudden decrease and rise amplitudes at certain frequency contents compared to the undamaged node.

Transfer functions technique was adopted in this study to determine the non-destructive performance level in the structure. Transfer functions were obtained by dividing the response of the damaged node by the earthquake input in the frequency domain and the response of the undamaged node by the damaged node (TF1). The transfer function (TF2) values of the damaged and undamaged nodes of the 1st floor and the transfer function (TF) of the undamaged node of the 2nd floor were obtained. It has been determined that damage levels increase as transfer function values increase. The fact that the transfer function curves are not complex and their values are low shows that the earthquake effects are dampened.

Figure 16, Transfer function values at the damaged node of the 1st floor are given. Figure 17 shows the transfer function values of the undamaged node of the 1st floor. In Figure 18, the transfer function values of the damaged node of the 2nd floor are given. Within the scope of intact state transfer functions, it is defined as low amplitudes at high frequency values or higher amplitudes at low frequency values compared to other frequency ranges. The damaged state is expressed as high transfer function amplitudes at high frequency values. It was found that the estimated transfer function value for the undamaged case was 10 on average.

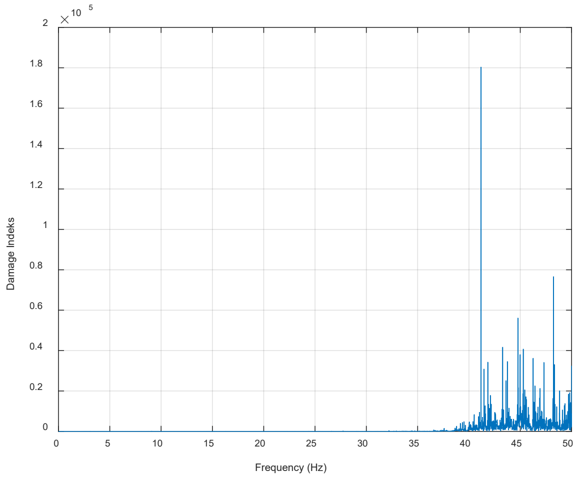

Figure 16. Damage structural frame in the first floor

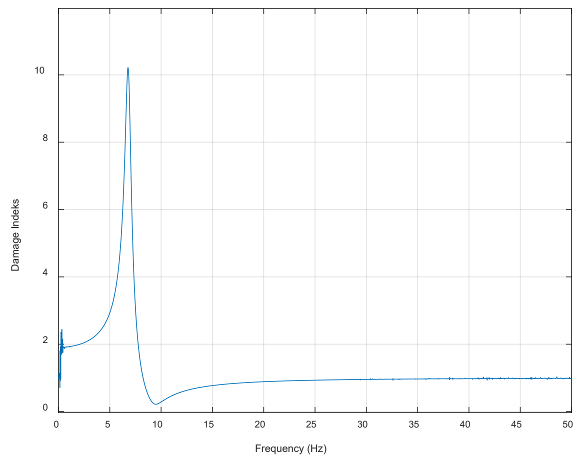

Figure 17. Non-damaged structural frame in the second floor

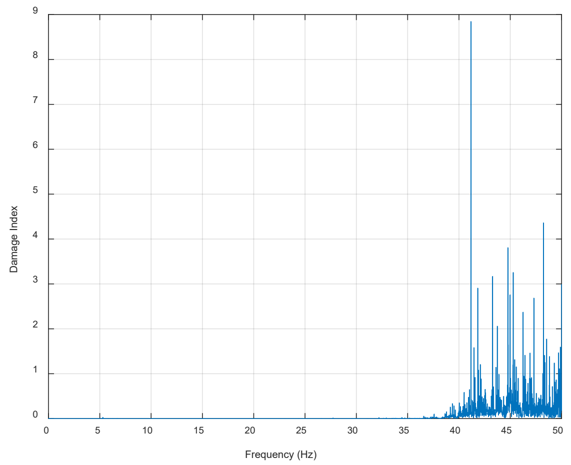

Figure 18. Non-damaged structural frame in the first floor

Declaration of Conflict of Interests

The authors declare that there is no conflict of interest. They have no known competing financial interests or personal relationships that could have appeared to influence the work reported in this paper.

References

[1.] Fragiacamo, M., Amadio, C.,Macorini, L., Seismic response of steel frames under repeated earthquake ground motions. Engineering Structures 26(13) (2004) 2021–2035.

[2.] FEMA 273 NEHRP Guidelines for the Seismic Rehabilitation of ... https://www.yumpu.com/en/document/view/51689942/fema-273-nehrp-guidelines-for-the-seismic-rehabilitation-of-. Accessed 17 Sep 2022a

[3.] ASCE 31 and 41. https://doi.org/10.1061/ASCE3141

[4.] TBEC 2018 Turkey Building Earthquake Code

[5.] Fragiadakis, M., Vamvatsikos, D., Aschheim, M., Application of nonlinear static procedures for the seismic assessment of regular rc moment frame buildings. Earthq Spectra 30(2)(2014)767–94.

[6.] Poursha, M., Khoshnoudian, F., Moghadam, A.S., Assessment of modal pushover analysis and conventional nonlinear static procedure with load distributions of Federal Emergency Management Agency for high-rise buildings. Journal of Structural Design of Tall and Special Buildings 19(3) (2010) 291–308.

[7.] Dya, A.F.C., Oretaa, A.W.C., Seismic vulnerability assessment of soft story irregular buildings using pushover analysis. Procedia Eng 125 2015 925–32.

[8.] Li, Y., Song, R., Van De Lindt, J.W. Collapse fragility of steel structures subjected to earthquake mainshock-aftershock sequences. J Struct Eng 140(12)2014 04014095.

[9.] Demirbaş, N., Durucan, c., Sahin, H., An energy-based method to calculate the vulnerability scores of RC buildings for rapid structural assessment methods. Structures 41 (2022) 147-158.

[10.] Kosarzadeh, H., Poursha, M., Seismic evaluation of vertically irregular RC frames subjected to mainshock-aftershock sequences of near-fault and far-fault ground motions. Structures 49 (2023) 1130-1156.

[11.] Kim, T., Park, J.H., Yu, E., Seismic fragility of low-rise piloti buildings based on 2017 Pohang earthquake damage. Journal of Building Engineering 76 (2023) 107032.

[12.] Zhou, P., Xiong, Z., Chen, X., Wang, J., Seismic performance of RC frame structure across the earth fissure based on pushover analysis. Structures 52 (2023) 1035-1050.

[13.] Peng, W.J., Li, A.Z., Tao, M.X., Evaluation and story drift ratio limits of structures with separated gravity- and lateral-load-resisting systems using pushover analysis. Journal of Building Engineering 76 (2023) 107223.

[14.] Yan, Y.J., Cheng, L., Wu, Z.Y., Yam, L.H., Development in vibration-based structural damage detection technique. Mech Syst Signal Process 21 (2007) 2198–211.

[15.] Ye, X.W., Dong, C.Z., Liu, T., A review of machine vision-based structural health monitoring: methodologies and applications. J Sens 2016.

[16.] Na, W.S, Baek, J., A review of the piezoelectric electromechanical impedance based structural health monitoring technique for engineering structures. Sens (Switz) 2018 18.

[17.] Li, H.N., Li, D.S., Song GB. Recent applications of fiber optic sensors to health monitoring in civil engineering. Eng Struct 26 (2004)1647–57.

[18.] Radzienski, ´ M., Krawczuk, M., Palacz, M., Improvement of damage detection methods based on experimental modal parameters. Mech Syst Signal Process 25 (2011) 2169–90.

[19.] Lam, H.F., Yin, T., Dynamic reduction-based structural damage detection of transmission towers: Practical issues and experimental verification. Eng Struct 33 2011 1459–78.

[20.] Panteliou, S., Chondros, T., Argyrakis, V., Dimarogonas, A., Damping factor as an indicator of crack severity. J Sound Vib 241 (2001) 235–45.

[21.] Ratcliffe, C., A frequency and curvature based experimental method for locating damage in structures. J Vib Acoust 122 (2000) 324–9.

[22.] Sohn, H., Farrar, C.R., Hemez, F.M., Shunk, D.D, Stinemates, D.W, Nadler, B.R., et al. A review of structural health monitoring literature: 1996–2001, Los Alamos National Laboratory report, (LA-13976-MS), 204).

[23.] Li, J., Law, S.S., Ding, Y., Substructure damage identification based on response reconstruction in frequency domain and model updating. Engineering Structures 41 (2012) 270-284.

[24.] Beyen, K., Damage ıdentification analyses of a historic masonry structure in T-F domain. Journal of Technical 604 (2021) 10577-10610.

[25.] Perez, A.M., More, J.F., Esmerats, J.F., Structural damage assessment in lattice towers based on a novel frequency domain-based correlation approach. Engineering Structures 226 (2021) 1132329.

[26.] Zhan, J., You, J., Kong, X., Zhang, N., An indirect bridge frequency identification method using dynamic responses of high-speed railway vehicles. Engineering Structures 243 (2021) 112694.

[27.] Song, Q., Li, Q., Thompson, D.J., Comparison of time-domain and frequency-domain models for vibration prediction of a rail transit viaduct paved with floating slab track. Engineering Structures 310 (2024) 118157.

[28.] TS498, İn dımensıonıng of buıldıng elements account values of loads to be purchased desıgn loads for buildings. Turkish Standart.1997.

[29.] AFAD T.R. Ministry of Internal Affairs, Disaster and Emergency Management Presidency, https://tadas.afad.gov.tr/

[30.] Rajasekaran, S., Structural dynamics of earthquake engineering. Boca Raton Boston New York Washington, DC. 2009.

[31.] Chopra, A., Dynamics of structures. Prentıce-Hall Internatıonal Series in Civil Engineering and Engineering Mechanics William J. Hall, Editor. 2012.

How to Cite This Article

Çelebi, O., Kılıç, M., Aydın, A.C., Damage Diagnosis in RC Frames on a Frequency Domain Basis, Civil Engineering Beyond Limits, 2(2024), 1927.
https://doi.org/10.36937/cebel.2024. 1927